HEAT AND MASS TRANSFER EFFECTS ON NATURAL CONVECTION FLOW ALONG A HORIZONTAL TRIANGULAR WAVY SURFACE

by

Sadia SIDDIQA[a*], M. Anwar HOSSAIN[b], and AQSA[c]

[a] Department of Mathematics, COMSATS Institute of Information Technology, Attock, Pakistan
[b] Department of Mathematics, University of Dhaka, Dhaka, Bangladesh
[c] Department of Mathematics, Quaid-e-Azam University, Islamabad, Pakistan

Original scientific paper
https://doi.org/10.2298/TSCI150722093S

An analysis is carried out to thoroughly understand the characteristics of heat and mass transfer for the natural convection boundary layer flow along a triangular horizontal wavy surface. Combine buoyancy driven boundary layer equations for the flow are switched into convenient form via co-ordinate transformations. Full non-linear equations are integrated numerically for Pr = 0.051. Interesting results for the uneven surface are found which are expressed in the form of wall shear stress, rate of heat transfer and rate of mass transfer. Solutions are also visualized via streamlines, isotherms, and isolines for concentration. Computational results certify that, shear stress, temperature gradient and concentration gradient enhances as soon as the amplitude of the wavy surface, a, increases, but complex geometry do not allow to carry simulations for a > 1.5. This factor probably ensures that sinusoidal waveform is better than triangular waveform.

Key words: *natural convection, triangular wavy surface, boundary layer, heat transfer, mass transfer*

Introduction

Sinusoidal wavy/uneven surfaces have gained considerable attention due to their ability to transmit more heat as compare to smooth surfaces. Experimentalists and engineers analyzed the behavior of uneven surfaces and found its applicability in solar collectors, condensers in refrigerators, cavity wall insulating systems, grain storage containers, and industrial heat radiators, *etc.* Flow behavior and heat transfer rate induced due to complex wavy surface was initially discussed by Yao [1] and Moulic and Yao [2, 3]. Later, considering the sinusoidal waveform, investigations on the natural convection flow as well as on the mixed convection flow of viscous fluid past or along wavy heated body of different shapes, such as vertical plate, horizontal plate, cylinder and cones have been accomplished by [4-16]. Besides this, some work has also been done by considering wavy surface of triangular form. Parvin *et al.* [17] studied the effect of MHD on mixed convection heat transfer through vertical wavy (sinusoidal and triangular) isothermal channels. They obtained the results numerically and examined the effect of several parameters in terms of streamlines, isotherms, and Nusselt number. Combined convection flow in triangular wavy chamber filled with water-CuO nanofluid was analyzed by Nasrin *et al.* [18]. In this study, authors displayed the effect of the Reynolds number, Richardson number, and the nanoparticles volume fraction on the flow and heat transfer characteristics in the cavity. Recently, Siddiqa *et al.* [19] examined natural convection

* Corresponding author, e-mail: saadiasiddiqa@gmail.com

flow of viscous fluid over triangular wavy horizontal surface. This was the first time that triangular wavy surface was discussed in the boundary layer region. The solutions were obtained numerically and comparison of sinusoidal and triangular form of wavy surface was done in terms of shear stress and rate of heat transfer.

However, it appears that the effect of combined buoyancy forces from mass and thermal diffusion over a triangular wavy surface has not been studied yet. The representative applications of combine mechanisms were initially studied by Gebhart and Pera [20] and Pera and Gebhart [21], along the vertical and horizontal surfaces, respectively, and later on plates with various orientations has been investigated, extensively. The details can be found in Gebhart *et al.* [22] and in Khair and Bejan [23], Lin and Wu [24, 25], Mongruel *et al.* [26], and Garooshi *et al.* [27]. In the current analysis, horizontal triangular wavy surface is considered over which double-diffusion effects on natural convection has been studied. Co-ordinate transformation (primitive variable formulations) are employed to transform the boundary layer equations into adjacent set of parabolic partial differential equations which are further integrated numerically by employing the implicit finite difference method that uses Thomas algorithm as a solver. Numerical results are obtained in terms of shear stress, rate of heat and mass transfer, velocity, temperature and concentration distributions and, also, envisioned through streamlines, isotherms and isolines (for concentration) for few parameters that occur while addressing the issue.

Analysis

Consider the 2-D boundary layer flow of a viscous incompressible fluid over a semi-infinite triangular wavy horizontal surface, which is driven by thermal and solutal buoyancy forces. The surface is maintained at a uniform temperature T_w and concentration C_w which are greater than the ambient fluid temperature T_∞ and C_∞, respectively. The fluid properties are assumed to be constant except for density variations, which induce buoyancy forces. The schematic diagram and co-ordinate system of the wavy pattern is:

$$\bar{\sigma}(\bar{x}) = \sum_{k=1}^{\infty} \frac{\alpha}{(2k-1)^2} \cos\left[\frac{(2k-1)\omega\bar{x}}{l}\right] \tag{1}$$

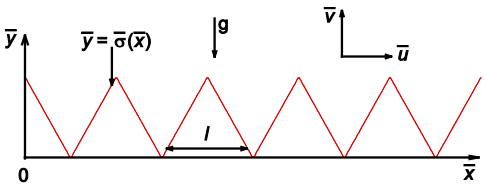

Figure 1. Physical model and the coordinate system

and is shown in fig. 1.

In eq. (1) α is the dimensional amplitude of the wavy surface, ω – the frequency of the wave, l – the characteristic length scale associated with the triangular waveform, and $\bar{x}$ – the Cartesian co-ordinate in the axial direction. The dimensionless governing boundary layer equations of continuity, momentum, energy and concentration under Boussinesq approximation are:

$$\frac{\partial u}{\partial x} + \frac{\partial v}{\partial y} = 0 \tag{2}$$

$$u\frac{\partial u}{\partial x} + v\frac{\partial u}{\partial y} = -\frac{\partial p}{\partial x} + \left(\frac{\partial^2 u}{\partial x^2} + \frac{\partial^2 u}{\partial y^2}\right) \tag{3}$$

$$u\frac{\partial v}{\partial x} + v\frac{\partial v}{\partial y} = -\frac{\partial p}{\partial y} + \left(\frac{\partial^2 v}{\partial x^2} + \frac{\partial^2 v}{\partial y^2}\right) + \mathrm{Gr}_T\,\theta + \mathrm{Gr}_C\,C \tag{4}$$

$$u\frac{\partial\theta}{\partial x}+v\frac{\partial\theta}{\partial y}=\frac{1}{\mathrm{Pr}}\left(\frac{\partial^2\theta}{\partial x^2}+\frac{\partial^2\theta}{\partial y^2}\right) \tag{5}$$

$$u\frac{\partial C}{\partial x}+v\frac{\partial C}{\partial y}=\frac{1}{\mathrm{Sc}}\left(\frac{\partial^2 C}{\partial x^2}+\frac{\partial^2 C}{\partial y^2}\right) \tag{6}$$

where

$$\overline{u}=\frac{\upsilon u}{l},\quad \overline{v}=\frac{\upsilon v}{l},\quad x=\frac{\overline{x}}{l},\quad y=\frac{\overline{y}}{l},\quad \overline{p}=\frac{\mu^2 p}{\rho l^2},\quad C=\frac{\overline{C}-C_\infty}{C_w-C_\infty},$$

$$\theta=\frac{\overline{T}-T_\infty}{T_w-T_\infty},\quad \mathrm{Pr}=\frac{\nu}{\overline{\alpha}},\quad \mathrm{Sc}=\frac{\nu}{\overline{D}},\quad \mathrm{Gr}_T=\frac{\mathrm{g}\beta_T(T_w-T_\infty)l^3}{\upsilon^2},\quad \mathrm{Gr}_C=\frac{\mathrm{g}\beta_C(C_w-C_\infty)l^3}{\upsilon^2}, \tag{7}$$

$$\overline{a}=\frac{\alpha}{l},\quad \overline{\sigma}=\frac{\sigma}{l},\quad \mathrm{Gr}=\mathrm{Gr}_T+\mathrm{Gr}_C$$

In eqs. (2)-(6), (*u, v*) are the dimensionless velocity components in the (*x*, *y*) directions, respectively, and are not parallel to nor perpendicular to the wavy surface, θ – the temperature of the fluid, C – the concentration, p – the pressure, $\overline{a}$ – the dimensionless amplitude of the wavy surface, ν – the kinematic viscosity, μ – the dynamitic viscosity, ρ – the density of the fluid, g – the acceleration due to gravity, β_T – the coefficient of volumetric expansion, β_C – the coefficient of concentration expansion, $\overline{\alpha}$ – the thermal diffusivity, Pr – the Prandtl number, Sc – the Schmidt number, Gr_T – the Grashof number for thermal diffusion, Gr_C – the Grashof number for mass diffusion, and $\overline{D}$ – the mass diffusivity.

The boundary conditions to be satisfied are:

$$\begin{gathered}u[x,\sigma(x)]=v[x,\sigma(x)]=0,\quad \theta[x,\sigma(x)]=C[x,\sigma(x)]=1,\\ u(x,\infty)=p(x,\infty)=\theta(x,\infty)=C(x,\infty)=0\end{gathered} \tag{8}$$

The effect of wavy surface is incorporated into the governing equations by using the following continuous transformations:

$$\begin{gathered}u=\mathrm{Gr}^{2/5}\,\xi^{1/5}U(\xi,\eta),\quad v=\mathrm{Gr}^{1/5}\,\xi^{-2/5}V(\xi,\eta),\quad p=\mathrm{Gr}^{4/5}\,\xi^{2/5}\varphi(\xi,\eta),\quad \theta=\theta(\xi,\eta),\\ C=C(\xi,\eta),\quad \eta=\mathrm{Gr}^{1/5}\,\xi^{-2/5}[y-\sigma(\xi)],\quad \overline{a}=\mathrm{Gr}^{-1/5}\,a,\quad x=\xi\end{gathered} \tag{9}$$

Substituting the previous transformations in eqs. (2)-(6) and in boundary conditions given in (8), we get:

$$\frac{U}{5}+\xi\frac{\partial U}{\partial\xi}-\left(\frac{2\eta}{5}+\xi^{3/5}\sigma_\xi\right)\frac{\partial U}{\partial\eta}+\frac{\partial V}{\partial\eta}=0 \tag{10}$$

$$\frac{U^2}{5}+\xi U\frac{\partial U}{\partial\xi}+\left[V-\left(\frac{2\eta}{5}+\xi^{3/5}\sigma_\xi\right)U\right]\frac{\partial U}{\partial\eta}+\xi\frac{\partial\varphi}{\partial\xi}+\frac{2\varphi}{5}-\left(\frac{2\eta}{5}+\xi^{3/5}\sigma_\xi\right)\frac{\partial\varphi}{\partial\eta}=\frac{\partial^2 U}{\partial\eta^2} \tag{11}$$

$$\frac{\partial\varphi}{\partial\eta}=\frac{\theta+NC}{1+N} \tag{12}$$

$$\xi U\frac{\partial\theta}{\partial\xi}+\left[V-\left(\frac{2\eta}{5}+\xi^{3/5}\sigma_{\xi}\right)U\right]\frac{\partial\theta}{\partial\eta}=\frac{1}{\mathrm{Pr}}\frac{\partial^2\theta}{\partial\eta^2} \tag{13}$$

$$\xi U\frac{\partial C}{\partial\xi}+\left[V-\left(\frac{2\eta}{5}+\xi^{3/5}\sigma_{\xi}\right)U\right]\frac{\partial C}{\partial\eta}=\frac{1}{\mathrm{Sc}}\frac{\partial^2 C}{\partial\eta^2} \tag{14}$$

Boundary conditions are:

$$\begin{gathered}U(\xi,0)=V(\xi,0)=0,\qquad \theta(\xi,0)=C(\xi,0)=1,\\ U(\xi,0)=p(\xi,0)=\theta(\xi,0)=C(\xi,0)=0\end{gathered} \tag{15}$$

where the parameter $N = \mathrm{Gr}_C/\mathrm{Gr}_T$ measures the relative effects between buoyancy forces, which arises from the mass diffusion and the thermal diffusion. It can be noted that N is taken to be zero for the case of no species diffusion, positive for measuring the combined influence of thermal and species diffusion, negative for observing the opposite effects of both and of infinite magnitude for having no thermal diffusion. It is further observed that for purely horizontal surface case ($a = 0.0$), the underlying problem reduces to the model discussed by Pera and Gebhart [21]. Recent analysis of Siddiqa *et al.* [19] also becomes the special case of the current study. In [19], authors only studied the effect of heat transfer; therefore, this analysis serves as an extension of [19] and the results of [19] can be retrieved by setting buoyancy ratio parameter $N = 0.0$.

Numerical method

The system of eqs. (10)-(14) are highly non-linear; no closed form analytical solutions could be obtained. Therefore, numerical solutions are obtained for the coupled non-linear partial differential eqs. (10)-(14) under the boundary conditions (15) by using an implicit, iterative tri-diagonal finite difference scheme similar to that of Blotter [28]. All the first order derivatives with respect to ξ are replaced by two-point backward difference formulae of the form:

$$\left(\frac{\partial\Omega}{\partial\xi}\right)_{i,j}=\frac{\Omega_{i,j}-\Omega_{i-1,j}}{\Delta\xi} \tag{16}$$

Similarly, derivatives with respect to η are replaced by central difference quotients of the form:

$$\left(\frac{\partial\Omega}{\partial\eta}\right)_{i,j}=\frac{\Omega_{i,j+1}-\Omega_{i,j-1}}{2\Delta\eta} \tag{17}$$

where

$$\begin{gathered}\Omega_{i,j}=\Omega(\xi_i,\eta_j),\quad \eta_j=(j-1)\Delta\eta\quad \text{for}\quad j=1,2,\ldots,K,\\ \eta_\infty=\eta_K,\quad \xi_i=(i-1)\Delta\xi\quad \text{for}\quad i=1,2,\ldots,M\end{gathered} \tag{18}$$

Here $\Omega_{i,j}$ denotes the dependent variable U, θ, φ, and C, and i, j are the node locations along the ξ and η directions, respectively. Therefore, system of partial differential equations is transformed to the system of algebraic equations. At each line of constant ξ, a system of algebraic equations is obtained. The non-linear terms are evaluated at the previous iteration

via implicit finite difference scheme for the numerical integration of tri-diagonal matrix. The system of algebraic equations is cast into a tridiagonal matrix equation of the form:

$$D_j\omega_{j-1} + E_j\omega_j + F_j\omega_{j+1} = G_j \tag{19}$$

where

$$\omega_j = \begin{bmatrix} U \\ \varphi \\ \theta \\ C \end{bmatrix}_{i,j}, \quad D_j = \begin{bmatrix} D_{11} & 0 & 0 & 0 \\ 0 & D_{22} & 0 & 0 \\ 0 & 0 & D_{33} & 0 \\ 0 & 0 & 0 & D_{44} \end{bmatrix}_{i,j}, \quad E_j = \begin{bmatrix} E_{11} & E_{12} & E_{13} & E_{14} \\ 0 & E_{22} & E_{23} & E_{24} \\ 0 & 0 & E_{33} & E_{34} \\ 0 & 0 & 0 & E_{44} \end{bmatrix}_{i,j},$$
$$F_j = \begin{bmatrix} F_{11} & 0 & 0 & 0 \\ 0 & F_{22} & 0 & 0 \\ 0 & 0 & F_{33} & 0 \\ 0 & 0 & 0 & F_{44} \end{bmatrix}_{i,j}, \quad G_j = \begin{bmatrix} G_1 \\ G_2 \\ G_3 \\ G_4 \end{bmatrix}_{i,j}, \quad \omega_1 = \begin{bmatrix} 0 \\ \varphi(1,1) - \Delta\eta \\ 1 \\ 1 \end{bmatrix}, \quad \omega_K = \begin{bmatrix} 0 \\ 0 \\ 0 \\ 0 \end{bmatrix} \tag{20}$$

An algorithm that can be used to obtain the solution ω_j at a certain stream-wise distance ξ, *i. e.*, for a particular value of M is [28]:

$$\omega_j = -H_j\omega_{j+1} + J_j, \qquad 1 \le j \le K-1 \tag{21}$$

where

$$H_1 = H_K = \begin{bmatrix} 0 & 0 & 0 & 0 \\ 0 & 0 & 0 & 0 \\ 0 & 0 & 0 & 0 \\ 0 & 0 & 0 & 0 \end{bmatrix}, \quad J_1 = \begin{bmatrix} 1 \\ 1 \\ 1 \\ 1 \end{bmatrix}, \quad J_K = \begin{bmatrix} 0 \\ 0 \\ 0 \\ 0 \end{bmatrix},$$
$$H_j = (E_j - D_jH_{j-1})^{-1}F_j \quad \text{for} \quad 2 \le j \le K-1, \tag{22}$$
$$J_j = (E_j - D_jH_{j-1})^{-1}(G_j - D_jJ_{j-1}) \quad \text{for} \quad 2 \le j \le K-1$$

Based on the information available at the i^{th} nodal point, the dependent variables ω_j are predicted at $i+1^{\text{th}}$ stage by adopting the following procedure.

(1) The values of the matrix elements D_j, E_j, F_j, G_j, are calculated using the known values of the unknown variables at i.

(2) Further, by using the iterative procedure given in (21) and (22), the H_j and J_j based on the values of the variables at i are calculated for all j ranging from 1 and K, starting at the surface $j = 1$ and values of H_j and J_j in (21) and using the conditions H_1, H_K, J_1, J_K given in (22), the values of the dependent variables $\Omega_{i,j}$ at $i + 1$ nodal point are determined in the reverse order (backward substitution), *i. e.*, starting from $j = K$.

(3) The computations are iterated until the unknown quantities meet the convergence criteria at the streamwise position. The convergence criteria is:

$$\max|U_{i,j}| + \max|V_{i,j}| + \max|\theta_{i,j}| + \max|\varphi_{i,j}| + \max|C_{i,j}| \le 10^{-6}$$

(4) Steps 2-3 are repeated for ξ maximum.

In the computation, continuity equation is used to obtain normal velocity component V by using the following discretization:

$$V_{i,j} = V_{i,j-1} - \frac{U_{i,j}}{5}\Delta\eta + U_{i,j}\left[\left(\frac{2\eta}{5} + \xi^{3/5}\sigma_\xi\right) - \xi\frac{\Delta\eta}{\Delta\xi}\right] + \\ + \left[\xi\frac{\Delta\eta}{\Delta\xi}U_{i-1,j} - \left(\frac{2\eta}{5} + \xi^{3/5}\sigma_\xi\right)U_{i,j-1}\right] \tag{23}$$

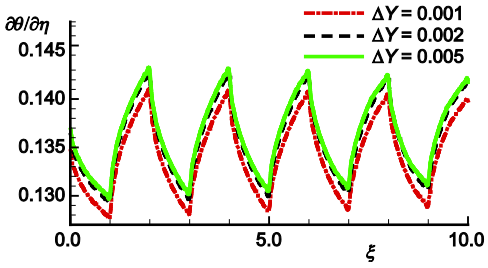

Figure 2. Grid independent test by taking $\Delta\eta$ = 0.001, 0.002, 0.005 while a = 0.1, N = 0.5, $\omega = \pi$, Pr = 0.051, and Sc = 2.0

In the cross streamwise direction, η, 25001 uniform grid points are employed. Additionally, there are 2501 grid points in the marching direction. In the program test, a finer axial step size, $\Delta\xi$ = 0.006, is tried and found to give acceptable accuracy. The computation has been started from ξ = 0.0 and then it marched up to ξ = 15.0 by taking uniform grids. In order to find the optimal grid size, different values of $\Delta\eta$ are tested. The values are plotted for a range of various $\Delta\eta$ (0.005, 0.002, 0.001) in fig. 2 and it is observed that the optimal value for which solutions become independent of grid size is $\Delta\eta \leq 0.002$. After comparing the results for different grid sizes in η direction, we choose $\Delta\eta$ = 0.002 and the value of the edge of the boundary layer η_∞ is 50.0 which actually correspond to the condition $\eta \to \infty$. It is further noticed that each execution of the FORTRAN code typically takes 38.5 CPU minutes.

The quantities of physical interest are: surface shear stress, the rate of heat transfer and the rate of mass transfer which may be attained with the help of following relations:

$$C_f \mathrm{Gr}^{-3/5}\ \xi^{1/5}(1+\sigma_\xi^2)^{-1} = \left(\frac{\partial U}{\partial\eta}\right)_{\eta=0}, \qquad \mathrm{Nu}\mathrm{Gr}^{-1/5}\xi^{2/5}(1+\sigma_\xi^2)^{-1/2} = -\left(\frac{\partial\theta}{\partial\eta}\right)_{\eta=0}, \\ \mathrm{Sh}\ \mathrm{Gr}^{-1/5}\ \xi^{2/5}(1+\sigma_\xi^2)^{-1/2} = -\left(\frac{\partial C}{\partial\eta}\right)_{\eta=0} \tag{24}$$

The following section contains the solutions obtained in terms of the previously mentioned quantities. Particularly the effect of amplitude of the triangular wavy surface, a, and buoyancy ratio parameter, N, is discussed on shear stress, rate of heat and mass transfer, velocity, temperature and concentration profiles, streamlines, and isotherms and isolines (for concentration).

Numerical results and discussion

Present analysis is performed for double diffusion natural convection flow of viscous fluid over a semi-infinite triangular wavy surface of the form given in eq. (1). Consideration is given to liquid metals and particularly Prandtl number is set to be 0.051 throughout the analysis. The certain range of non-dimension variables is chosen for numerical simulation, which are dictated by the values appeared in the existing literature so that wherever possible, the present results for special cases could be compared with existing results. Taking cognizance of the published results of Siddiqa *et al.* [19], it follows that, present results can be compared with their solutions by setting amplitude of the triangular wavy surface a = 0.0 and buoyancy ratio parameter N = 0.0. This comparison is done in terms of values of $U'(0)$ and

$\theta'(0)$ in tab. 1 for Prandtl number ranging from 0.01 to 7.0. It is observed that present results are in good agreement when compared with [19].

Table 1. Values of $U'(0)$ and $\theta'(0)$ for $a = 0.0$, $N = 0.0$

Pr	Siddiqa *et al.* [19]	Present	Siddiqa *et al.* [19]	Present
	$U'(0)$		$\theta'(0)$	
0.01	3.92182	3.92152	–	–
0.1	2.02721	2.02704	–	–
0.7	0.98733	0.98722	–	–
1.0	0.86129	0.86121	0.39042	0.39031
7.0	0.41340	0.41310	–	–

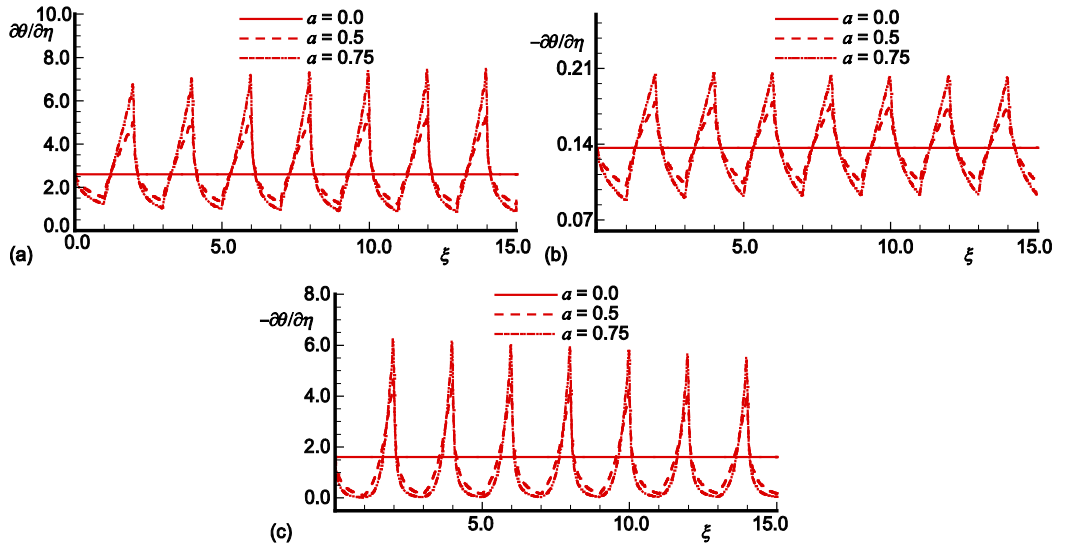

Figure 3. Variation of (a) wall shear stress, (b) rate of heat transfer, (c) rate of mass transfer for $a = 0.0$, 0.5, and 0.75, $N = 0.5$, $\omega = \pi$, Pr = 0.051, and Sc = 10.0

The impact of amplitude of the horizontal wavy surface, a, is noted on shear stress, rate of heat transfer and rate of mass transfer in fig. 3. Graphical representation is given for $a = 0.0$, 0.5, and 0.75 against the axial distance ξ particularly for Pr = 0.051, $\omega = \pi$, Sc = 10.0, and $N = 0.5$. It can be noted that Pr $\ll$ Sc, which ensures that, results are obtained for liquid metals. Here Prandtl number is small, which is responsible in enhancement of thermal conductivity that quickly diffuses away the heat from the uneven surface. The graphs for $a = 0.0$ retrieve the results for purely horizontal smooth plate. The figure ensures that shear stress, temperature gradient and concentration gradient get stronger in the vicinity of the plate for $a > 0.0$. It happens because of the influence of centrifugal force and buoyancy forces. Therefore, stronger the amplitude of the wavy surface, higher will be the wall shear stress and heat and mass transfer. Further, fig. 3(c) delivers spike-like waves that find its applications in engineering.

The effect of buoyancy ratio parameter N is shown in fig. 4 for $N = -0.1$, 0.0, 0.1, and 5.0, $\omega = \pi$, $a = 0.5$, Pr = 0.051, and Sc = 2.0. Specifically, $N = 0.0$ represents the case

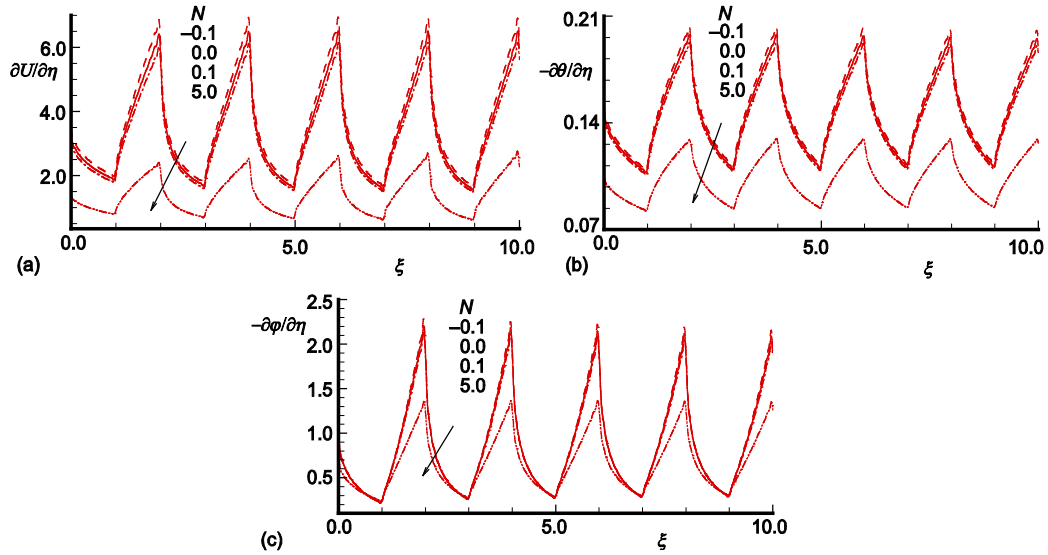

Figure 4. Variation of (a) wall shear stress, (b) rate of heat transfer, (c) rate of mass transfer for N = –0.1, 0.0, 0.1, and 5.0, $\omega = \pi$, a = 0.5, Pr = 0.051, and Sc = 2.0

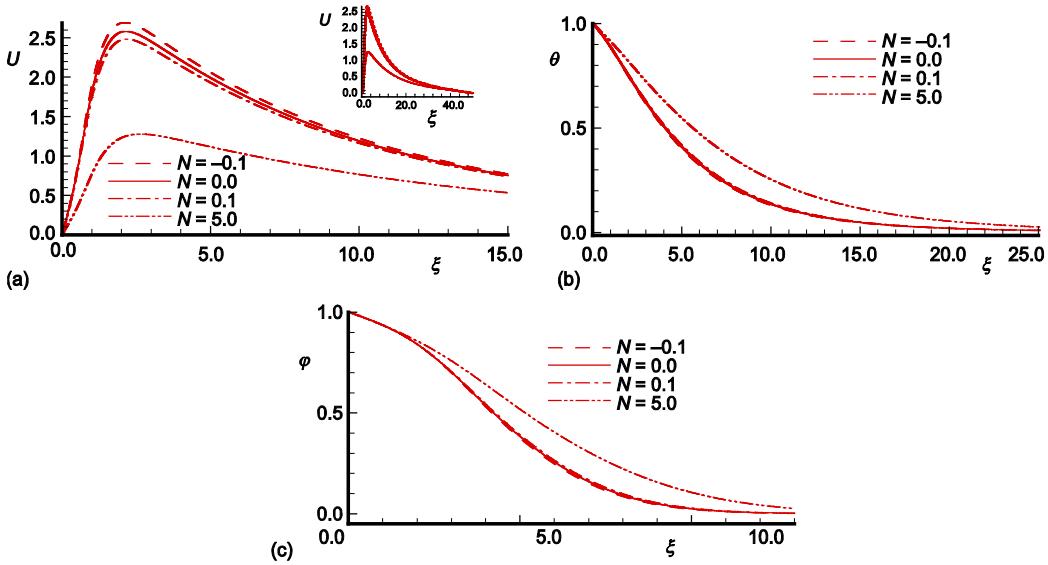

Figure 5. (a) velocity, (b) temperature, and (c) concentration profiles for N = –0.1, 0.0, 0.1, and 5.0, a = 0.5, $\omega = \pi$, Pr = 0.051, and Sc = 2.0

when species diffusion is absent and the flow is induced entirely by thermal effects. The momentum equation is then de-coupled from the species concentration equation and this result actually recovers the solution set of Siddiqa *et al.* [19]. However, $N > 0.0$ (aiding flow) refers to the case when both thermal and species diffusion are present and $N = –1.0$ (opposing flow) ensures that the mass buoyancy force acts in the opposite direction of thermal buoyancy force. It is reported that gradients of velocity, temperature, and concentration tends to decrease as N increases from –1.0 to 5.0.

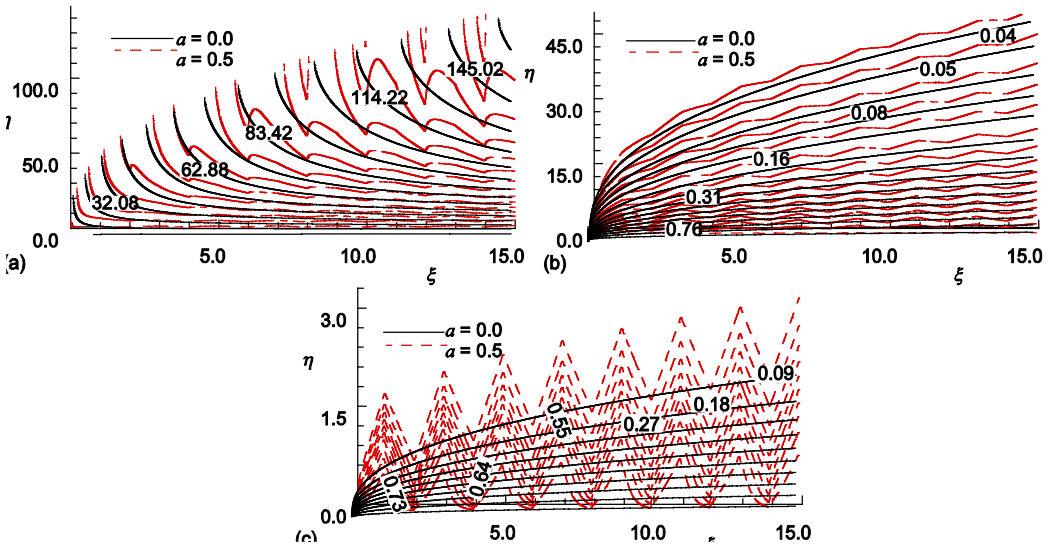

Figure 6. Variation of (a) streamlines, (b) isotherms, and (c) isolines for concentration for a = 0.0, 0.5, N = 0.5, $\omega = \pi$, Pr = 0.051, and Sc = 10.0

Velocity, temperature, and concentration profiles are also plotted in fig. 5 for various values of buoyancy ratio parameter N. It is found that, except velocity, temperature and concentration profiles increases, when N tends to increase. Therefore, in case of velocity, thermal and solutal forces make opposing contribution of each other. However, the enhancement of non-dimensional temperature and concentration profiles is due to the reduction in the thickness of thermal and concentration boundary layers, respectively.

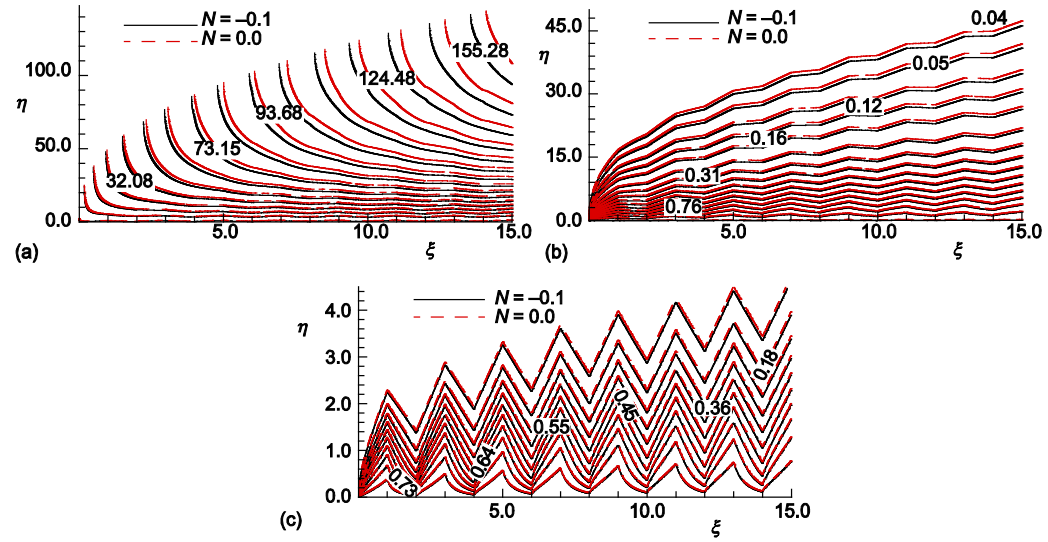

Figure 7. Variation of (a) streamlines, (b) isotherms, and (c) isolines for concentration for N = –0.1, 0.0, a = 0.5, $\omega = \pi$, Pr = 0.051, and Sc = 2.0

Further, streamlines and isotherms are also drawn for important physical parameters in order to get the pattern of the fluid flow. In fig. 6 the influence of amplitude of the triangular wavy surface, a, is shown in the form of streamlines, isotherms, and isolines for concentration for $\xi \in [0, 15]$. Result are plotted for two values of a, whilst Pr = 0.051, Sc = 10.0, $N = 0.5$, and $\omega = \pi$. The interpretation of the results is already discussed earlier, however, the distribution of velocity, temperature and concentration in the boundary layer region can be observed in figs. 6(a)-(c). Clearly, waviness has pronounced effect on isolines for concentration. Similarly, the variation of N is depicted in terms of streamlines, isotherms, and isolines for concentration in fig. 7. This figure also brief about the behavior of momentum transfer, heat transfer, and mass transfer.

Conclusions

This paper aims to compute numerical results of natural convection flow of a viscous fluid over a horizontal triangular wavy surface. The coupled non-linear governing equations of fluid flow, heat transfer and species concentration are solved via implicit finite difference scheme. Results are obtained and interpreted for Pr $\ll$ Sc. Variation of specific parameters is shown in terms of shear stress, heat and mas transfer rate, velocity, temperature and concentration distributions and streamlines, isotherms, and isolines (for concentration). The behavior of amplitude of the wavy surface, a, is observed in the presence of species concentration and it is established that physical quantities are more escalating for higher value of a. The present results also help in concluding the fact that buoyancy ratio parameter, N, do not promote any of the physical quantity given in eq. (24).

References

[1] Yao, L. S., Natural Convection along a Vertical Wavy Surface, *ASME Journal of Heat Transfer*, *105* (1983), 3, pp. 465-468
[2] Moulic, S. G., Yao, L. S., Natural Convection along a Wavy Surface with Uniform Heat Flux, *ASME Journal of Heat Transfer*, *111* (1989), 4, pp. 1106-1108
[3] Moulic, S. G., Yao, L. S., Mixed Convection along Wavy Surface, *ASME Journal of Heat Transfer*, *111* (1989), 4, pp. 974-979
[4] Rees, D. A. S., Pop, I., Free Convection Induced by a Horizontal Wavy Surface in a Porous Medium, *Fluid Dynamics Research*, *14* **(**1994**)**, 4, pp. 151-166
[5] Hossain, M. A., Pop, I., Magnetohydrodynamic Boundary Layer Flow and Heat Transfer on a Continuous Moving Wavy Surface, *Archives of Mechanics*, *48* (1996), 5, pp. 813-823
[6] Hossain, M. A., Rees, D. A. S., Combined Heat and Mass Transfer in Natural Convection Flow from a Vertical Wavy Surface, *Acta Mechanica*, *136* (1999), 3, pp. 133-141
[7] Hossain, Md. A., *et al.*, Natural Convection with Variable Viscosity and Thermal Conductivity from a Vertical Wavy Cone, *International Journal of Thermal Sciences*, *40* (2001), 5, pp. 437-443
[8] Jang, J. H., Yan, W. M., Mixed Convection Heat and Mass Transfer along a Vertical Wavy Surface, *International Journal of Heat and Mass Transfer*, *47* (2004), 3, pp. 419-428
[9] Molla, M. M., Hossain, M. A., Radiation Effect on Mixed Convection Laminar Flow along a Vertical Wavy Surface, *International Journal of Thermal Sciences, 46* (2007), 9, pp. 926-935
[10] Molla, M. M., *et al.*, Natural Convection Flow along a Vertical Complex Wavy Surface with Uniform Heat Flux, *ASME Journal of Heat Transfer*, *129* (2007), 10, pp. 1403-1407
[11] Yau, H.-T., *et al.*, A Numerical Investigation into Electroosmotic Flow in Microchannels with Complex Wavy Surfaces, *Thermal Science*, *15* (2011), Suppl. 1, pp. S87-S94
[12] Narayana, M., *et al.*, On Double-Diffusive Convection and Cross Diffusion Effects on a Horizontal Wavy Surface in a Porous Medium, *Boundary Value Problems*, *2012* (2012), 1, pp. 1-22
[13] Siddiqa, S., Hossain, M. A., Natural Convection Flow over Wavy Horizontal Surface, *Advances in Mechanical Engineering*, *2013* (2013), Jan., ID 743034

[14] Bahaidarah, H. M. S., Sahin, A. Z., Thermodynamic Analysis of Fluid Flow in Channels with Wavy Sinusoidal Walls, *Thermal Science*, *17* (2013), 3, pp. 813-822
[15] Siddiqa, S., *et al.*, The Effect of Thermal Radiation on the Natural Convection Boundary Layer Flow over a Wavy Horizontal Surface, *International Journal of Thermal Sciences*, *84* (2014), Oct., pp. 143-150
[16] Xiaohong, G., *et al.*, Analysis of Three Dimensional Flow and Heat Transfer in a Cross Wavy Primary Surface Recuperator for a Microturbine System, *Thermal Science*, *19* (2015), 2, pp. 489-496
[17] Parvin, S., *et al.*, MHD Mixed Convection Heat Transfer through Vertical Wavy Isothermal Channels, *International Journal of Energy and Technology*, *3* (2011), 34, pp. 1-9
[18] Nasrin, R., *et al.*, Combined Convection Flow in Triangular Wavy Chamber Filled with Water-CuO Nanofluid: Effect Of Viscosity Models, *International Communications in Heat and Mass Transfer*, *39* (2012), 8, pp. 1226-1236
[19] Siddiqa, S., *et al.*, Natural Convection Flow of Viscous Fluid over Triangular Wavy Horizontal Surface, *Computers & Fluids*, *106* (2015.), Jan., pp. 130-134
[20] Gebhart, B., Pera, L., The Nature of Vertical Natural Convection Flows Resulting from the Combined Buoyancy Effects of Thermal and Mass-Diffusion, *International Journal of Heat and Mass Transfer*, *14* (1971), 12, pp. 2025-2050
[21] Pera, L., Gebhart B., Natural Convection Flows Adjacent to Horizontal Surfaces Resulting from the Combined Buoyancy Effects of Thermal and Mass Diffusion, *International Journal of Heat and Mass Transfer*, *15* (1972), 2, pp. 269-278
[22] Gebhart, B., *et al.*, *Buoyancy-Induced Flow and Transport*, Hemisphere Publ. Corp., Washington DC, USA, 1988
[23] Khair, K. R., Bejan, A., Mass Transfer to Natural Convection Boundary Layer Flow Driven by Heat Transfer, *ASME Journal of Heat Transfer*, *107* (1985), 4, pp. 979-981
[24] Lin, H. T., Wu, C.-M., Combined Heat Transfer by Laminar Natural Convection from a Vertical Plate, *Heat and Mass Transfer*, *30* (1995), 6, pp. 369-376
[25] Lin, H. T., Wu, C.-M., Combined Heat and Mass Transfer by Laminar Natural Convection from a Vertical Plate with Uniform Heat Flux and Concentrations*, Heat and Mass Transfer*, *32* (1997), 4, pp. 293-299
[26] Mongruel, A., *et al.*, Scaling of Boundary Layer Flows Driven by Double- Diffusive Convection*, International Journal of Heat and Mass Transfer*, *39* (1996), 18, pp. 3899-3910
[27] Garooshi, F., *et al.*, Two-Phase Mixture Modeling of Mixed Convection of Nanofluids in a Square Cavity with Internal and External Heating, *Powder Technology*, *275* (2015), May, pp. 304-321
[28] Blotter, F. G., Finite Difference Method of Solution of Boundary Layer Equations, *AIAA Journal*, *8* (1970), 2, pp. 193-205

Paper submitted: July 22, 2015
Paper revised: March 22, 2016
Paper accepted: April 23, 2016